

Title	Energy dissipation below gamma-ray bursts photosphere: evidence and spectral fits
Authors	Pe'er, Asaf
Publication date	2015-07
Original Citation	Pe'er, A. (2015) 'Energy dissipation below gamma-ray bursts photosphere: evidence and spectral fits', Proceedings of the Fourteenth Marcel Grossmann Meeting on General Relativity, Rome, Italy, 12-18 July, pp. 2943-2949. Available at: <a href="https://doi.org/10.1142/10614">https://doi.org/10.1142/10614</a> (Accessed 25 January 2019)
Type of publication	Conference item
Link to publisher's version	<a href="https://doi.org/10.1142/10614">https://doi.org/10.1142/10614</a>
Rights	© 2015, Asaf Pe'er. This paper is distributed under the terms of the Creative Commons Attribution 4.0 (CC BY) License. Further distribution of this work is permitted, provided the original work is properly cited. - <a href="https://creativecommons.org/licenses/by/4.0/">https://creativecommons.org/licenses/by/4.0/</a>
Download date	2025-03-18 23:20:23
Item downloaded from	<a href="https://hdl.handle.net/10468/7361">https://hdl.handle.net/10468/7361</a>

# Energy dissipation below gamma-ray bursts photosphere: Evidence and spectral fits

Asaf Pe'er\*

*Physics Department, University College Cork,  
Cork, Ireland*

*\* E-mail: a.peer@ucc.ie*

It is now established that a thermal emission component plays a major role in shaping the prompt spectra of a non-negligible fraction of gamma-ray bursts (GRBs). By studying the properties of this component in a sample of 47 GRBs, we deduce that the Lorentz factor is  $10^2 \lesssim \Gamma \lesssim 10^3$ , with mean value  $\langle \Gamma \rangle \simeq 370$ . The acceleration radius  $r_0$  span a wide range,  $10^{6.5} \lesssim r_0 \lesssim 10^{9.5}$  cm, with mean value  $\langle r_0 \rangle \simeq 10^8$  cm. This is higher than the gravitational radius of  $10 M_\odot$  black hole by a factor of  $\approx 30$ . We argue that this result provides an indirect evidence for jet propagation inside a massive star, and suggests the existence of recollimation shocks that take place at this radius. We further show that sub-photospheric dissipation of the jet kinetic energy provides a self-consistent, fully physically motivated model that can fit a wide range of GRB spectra. The leading radiative process is Comptonization of the thermal component, and synchrotron emission is sub-dominant. We create a DREAM (Dissipation with Radiative Emission as a Table Model) table model for XSPEC, and show how this model can describe different types of GRB spectra.

*Keywords:* Gamma-rays: bursts; hydrodynamics; radiation mechanism: non-thermal; radiation mechanism: thermal.

## 1. Introduction

One of the major developments in the study of gamma-ray bursts (GRBs) in recent years has been the realization that a thermal component may be a key spectral ingredient. As the shape of most GRB spectra do not resemble a Planck function, it is traditionally fitted with a simple mathematical function - a broken power law, known as the “Band” function<sup>1</sup>. Being mathematical in nature, it is very difficult to deduce physical information on the nature of GRBs from these fits. A breakthrough occurred about a decade ago, with the introduction of time-resolved spectral analysis<sup>2,3</sup>, and the realization that part of the over all non-thermal spectra in a non-negligible minority of GRBs<sup>4</sup> is consistent with having a black-body (“Planck”) shape that accompanies the non-thermal part.

Following the initial discovery, such a component was recently found in several Fermi GRBs as well, e.g.<sup>5-9</sup>. Since the ability to detect this component, as well as its significance depends on the analysis method - the “Band” model, for example, contains only four free parameters, and as such is unable to capture a weak thermal component<sup>10,11</sup>, it is possible that it is very ubiquitous. In fact, indirect evidence suggest that it exists in nearly 100% of all GRBs<sup>12,13</sup>.

The ability of detecting a thermal component holds great promise. A thermal component originates from the photosphere, the inner most region from which any electromagnetic signal can reach the observer. Therefore, the properties of this component directly reveal the physical conditions at the photosphere, in those GRBs

in which it is directly detected. Furthermore, this component can significantly affect the non-thermal part of the spectrum, as the thermal photons serve as seed photons for inverse-Compton (IC) scattering by the non-thermal particles<sup>14–16</sup>.

## 2. Hydrodynamic properties of GRB outflows

Within the framework of the classical “fireball” model (e.g.<sup>17</sup>) in which magnetic energy is sub-dominant, the photospheric radius depends only on two parameters: the (kinetic) luminosity,  $L$  and the bulk Lorentz factor,  $\Gamma$  at this radius. The observed temperature weakly depends, in addition, on the acceleration radius,  $r_0$  which is the radius where the acceleration of plasma to relativistic (kinetic) motion begins (and therefore  $r_0 > r_g$ , where  $r_g$  is the gravitational radius). Thus, for bursts with known redshift, measurements of the temperature and flux are sufficient to determine the basic dynamical properties:  $r_0$ ,  $L$ ,  $\Gamma$  and  $r_{ph}$ <sup>18</sup>.

In order for these estimates to be reliable, two conditions must be met. First, the distance to the GRB needs to be known; and second, the observed thermal component should not be strongly distorted, e.g., by sub-photospheric dissipation. A third condition is that the magnetization parameter is small, so that the magnetic field is dynamically unimportant<sup>19,20</sup>. If this is not the case, the dynamical variables are coupled (see<sup>20</sup> for full treatment).

The number of GRBs which fulfill both conditions is still very limited. No more than several dozens GRBs show a clearly distinct, dominant thermal component, and the redshifts of many of those are unknown. However, as was recently pointed out<sup>21</sup>, the added uncertainty in estimating the value of  $r_0$  due to the unknown redshift is  $\lesssim 25\%$ , and that of  $\Gamma$  is  $\lesssim 75\%$ . These values are based on the pre-Swift GRB redshift distribution, which is typically at the range  $0.5 \lesssim z \lesssim 2.5$ <sup>22</sup>.

This realization enabled Ref. 21 to carry a dynamical analysis on a sample of 47 GRBs. These GRBs were divided into 3 categories. Category (I) contains 7 GRBs for which all conditions are fulfilled (in particular, their redshift is known); in category (II) there are 4 Fermi GRBs, whose thermal component is pronounced but their redshift is unknown; and in category (III) there are 36 GRBs detected by BATSE, whose thermal component is pronounced but their redshift is unknown.

The results of the analysis are presented in Figures 1 and 2. The analysis was carried under the assumption that the ratio of energy released in the explosion to the energy observed in  $\gamma$ -rays is  $Y = 2^{23,24}$ . As is presented in the figures, the range of values of the Lorentz factor is  $130 \leq \Gamma \leq 1200$ , with  $\langle \Gamma \rangle = 370$ , and that of the acceleration radius is  $4 \times 10^6 \leq r_0 \leq 2 \times 10^9$  cm, with  $\langle r_0 \rangle = 9.1 \times 10^7$  cm. No significant correlation between the values of these two parameters was found.

Perhaps the most interesting result is the large value of  $r_0$  found. An average value of  $\langle r_0 \rangle \sim 10^8$  cm corresponds to variability time  $\delta t = r_0/c \sim 3$  ms, fully consistent with the observed variability  $\geq 10$  ms (with average value  $\approx 500$  ms,<sup>25</sup>) seen in GRBs. However, this value is  $\approx 30$  times greater than the gravitational radii of  $10M_\odot$  black hole. Indeed, within the context of the GRB “collapsar” model<sup>26</sup>, the

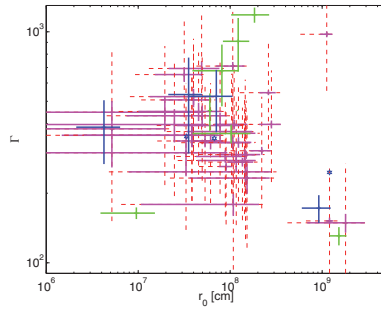


Fig. 1. Lorentz factor,  $\Gamma$ , vs acceleration radius,  $r_0$ , of GRBs in the sample of 47 GRBs<sup>21</sup>. Green, blue and magenta points are GRBs in categories (I), (II) and (III), respectively. Solid error bars represent statistical errors, while dashed error bars represent additional uncertainty due to unknown redshifts of category (III) GRBs. The stars show the location of the parameters of category (II) GRBs with assumed redshift  $z = 1$ . A linear fit reveals  $\Gamma \propto r_0^\alpha$  with  $\alpha = -0.10 \pm 0.09$  and a very weak correlation. The values of  $\Gamma$  and  $r_0$  presented are derived under the assumption  $Y = 2$ . For a different value of  $Y$ , the results can be scaled according to  $\Gamma \propto Y^{1/4}$  and  $r_0 \propto Y^{-3/2}$ .

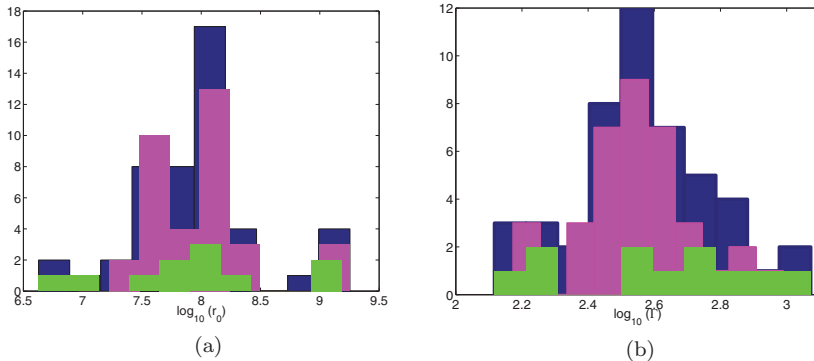


Fig. 2. Histograms of the mean values of  $\log_{10}(r_0)$  (left) and  $\log_{10}(\Gamma)$  (right). Blue are for the entire sample, while magenta are for GRBs in category (III) sample only (which is a homogeneous sub-sample), and green are for GRBs in categories (I) and (II).

collimated outflow within the collapsing star cannot be described as a free outflow. As the jet drills a funnel through the collapsing stellar material, it is confined by the funnel walls. During its propagation, the jet's thermal pressure decreases. If the external pressure decreases slower than the jet pressure, a recollimation shock must form. Thus, while the Lorentz factor increases up to the recollimation shock radius, there is a sharp drop in the outflow velocity as it encounters the recollimation shock to  $\Gamma \gtrsim 1$ , before the outflow re-accelerates above this radius. This is clearly seen in numerical models<sup>27–30</sup>. We can therefore conclude, that the results presented here imply that the large value of  $r_0$  may very well correspond to the location of the recollimation shock, and may therefore provide the first (indirect) evidence for the “collapsar” scenario.

### 3. Spectral fits of GRB prompt emission using sub-photospheric dissipation model

In addition to serving as a direct probe of the dynamics, thermal component is an important source of seed photons for Comptonization. This effect is pronounced if energy dissipation takes place close to the photosphere (one - two orders of magnitude below or above it). The dissipated energy, which can be either kinetic or magnetic is used, at least partially, to heat electrons to a temperature higher than that of the surrounding thermal photons. In such a scenario, the thermal photons are upscattered by the hot electrons. This leads to (I) rapid cooling of the hot electrons; for most reasonable parameter space region this means that the initial distribution of the electrons (e.g., power law or Maxwellian) have only a minor effect on the resulting spectra<sup>15</sup>; and (II) broadening of the “Planck” spectra. For a large parameter space region, the emerging spectra can resemble that of “Band” function<sup>16,31–33</sup>. Interestingly, in this scenario “Band”-like shapes are obtained in parameter space region where synchrotron emission is sub-dominant.

One important result is that the shape of the spectra is not very sensitive to the model uncertainties. Although the model has seven free parameters, the resulting spectral shape mainly depends on only two parameters: the radii (optical depths) in which the dissipation takes place, and the ratio of dissipated to thermal energy. A third parameter of somewhat less importance is the value of the magnetic field, that determines the synchrotron contribution.

While the theory is known for several years now, so far there had been very little use in it in fitting data. In order to bridge this gap, Ref 34 constructed a fully physically motivated model, called DREAM (*Dissipation with Radiation Emission as A table Model*). The physical scenario is based on the fireball model, while the radiation is treated using the code described in ref.<sup>35</sup>. The outcome of the radiative calculations are tabulated, and put as an input into *XSPEC*. This enables relatively fast fits, although the radiative calculations are relatively expensive.

The advantage of this work is demonstrated in Figures 3 and 4, which show fits to two GRBs: GRB090618 and GRB100724B. The spectra of these GRBs are qualitatively different. While GRB090618 can be well fitted by a “Band” function, GRB100724B requires the addition of another component, which can be interpreted as a black body (Planck). However, both spectra can be equally well fitted with the DREAM model. Fits with this model have the additional advantage that they provide the values of the physical ingredients to high accuracy. The spectra of GRB090618 is fitted with a model in which the dissipation occurs at optical depth  $\tau = 17 \pm 1.5$ , Lorentz factor  $\Gamma = 239 \pm 2$ , GRB luminosity  $L = 3.3 \pm 0.15 \times 10^{53}$  erg/s and fraction of dissipated kinetic energy  $\epsilon_d = 0.1$ . The statistical errors obtained using the DREAM model fits are the same magnitude as those obtained using the Band or Band + Planck fits.

## 4. Summary

Despite the fact that the spectra of the vast majority of GRBs do not resemble a “Planck” spectrum, the existence of a thermal component as part of an overall non-thermal spectra in many GRBs is now becoming widely accepted. This component may be the key ingredient needed to explain the dynamical properties and the spectral shape of GRBs. In those GRBs in which it is not or only weakly distorted, it provides direct probe of the dynamics; this is the case when energy dissipation (that is responsible for producing the non-thermal emission) does not occur close to the photosphere. On the other hand, in those GRBs in which energy dissipation does occur close to the photosphere, which may be the majority of GRBs, thermal component can play a key role in shaping the non-thermal part of the spectra, as the thermal photons serve as seed photons to IC scattering by the energetic electrons.

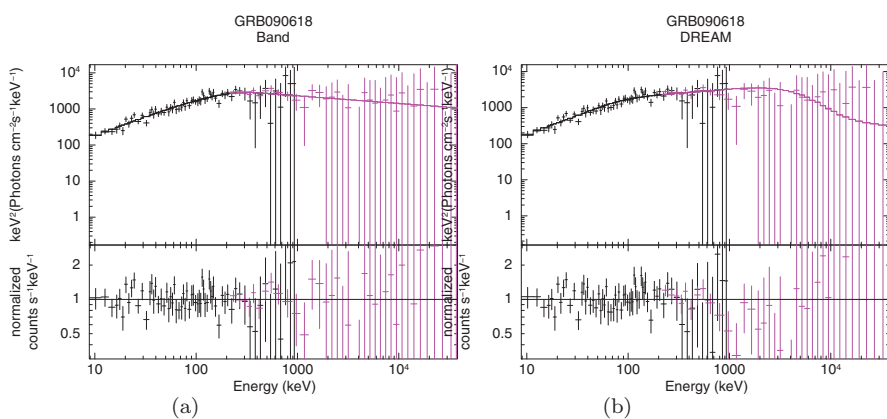


Fig. 3. Fits to GRB090618 at time bins 65.3-65.7 s. Left: fit with traditionally “Band” function. Right: Fit to the same data with DREAM model. See<sup>34</sup> for details.

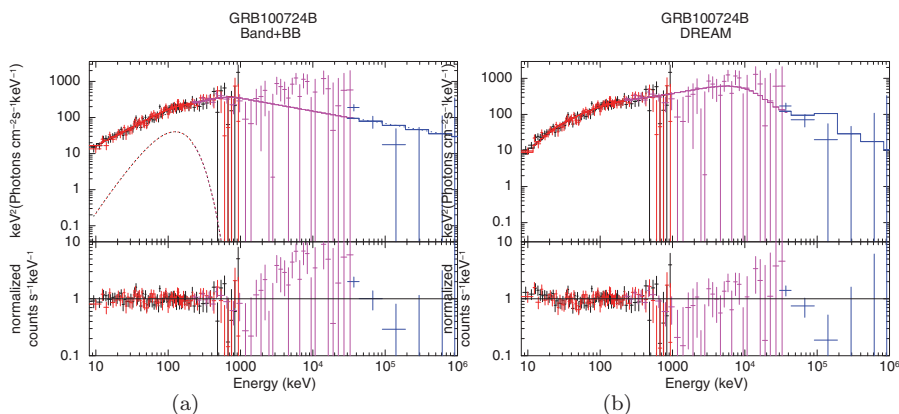


Fig. 4. Fits to GRB100724B at time bins 25.8-33.5 s. Left: fit with “Band” function plus black body. Right: Fit to the same data with DREAM model. See<sup>34</sup> for details.

With the accumulation of more data and the implementation of new fitting methods, such as the DREAM fits, a rapid advanced in our knowledge is guaranteed.

## Acknowledgments

The works described in this proceedings were carried in collaboration with Felix Ryde (KTH), Hugh Barlow (UCC), Shane O'Mahony (UCC), Björn Ahlgren (KTH), Raffaella Margutti (CfA), Josefin Larsson (KTH), Tanja Nymark (KTH), Davide Lazzati (Oregon State) and Mario Livio (STScI).

## References

1. D. Band, J. Matteson, L. Ford, et. al. *Astrophys. J.* **413**, 281(August 1993).
2. F. Ryde, *Astrophys. J.* **614**, 827(October 2004).
3. F. Ryde, *Astrophys. J.* **625**, L95(June 2005).
4. F. Ryde and A. Pe'er, *Astrophys. J.* **702**, 1211(September 2009).
5. F. Ryde, M. Axelsson, B. B. Zhang, S. McGlynn, A. Pe'er, et. al., *Astrophys. J.* **709**, L172(February 2010).
6. S. Guiriec, V. Connaughton, M. S. Briggs, M. Burgess, F. Ryde, et. al., *Astrophys. J.* **727**, p. L33(February 2011).
7. M. Axelsson, L. Baldini, G. Barbiellini, M. G. Baring, R. Bellazzini, et. al., *Astrophys. J.* **757**, p. L31(October 2012).
8. S. Iyyani, F. Ryde, M. Axelsson, J. M. Burgess, S. Guiriec, et. al., *Mon. Not. R. Astron. Soc.* **433**, 2739(August 2013).
9. S. Iyyani, F. Ryde, B. Ahlgren, J. M. Burgess, J. Larsson, A. Pe'er, C. Lundman, M. Axelsson and S. McGlynn, *Mon. Not. R. Astron. Soc.* **450**, 1651(June 2015).
10. S. Guiriec, C. Kouveliotou, F. Daigne, B. Zhang, R. Hascoët, et. al., *Astrophys. J.* **807**, p. 148(July 2015).
11. S. Iyyani, F. Ryde, J. M. Burgess, A. Pe'er and D. B\`egué, *ArXiv e-prints* (November 2015).
12. M. Axelsson and L. Borgonovo, *Mon. Not. R. Astron. Soc.* **447**, 3150(March 2015).
13. H.-F. Yu, H. J. van Eerten, J. Greiner, R. Sari, P. Narayana Bhat, A. von Kienlin, W. S. Paciesas and R. D. Preece, *Astron. Astrophys.* **583**, p. A129(November 2015).
14. M. J. Rees and P. Mészáros, *Astrophys. J.* **628**, 847(August 2005).
15. A. Pe'er, P. Mészáros and M. J. Rees, *Astrophys. J.* **635**, 476(December 2005).
16. A. Pe'er, P. Mészáros and M. J. Rees, *Astrophys. J.* **642**, 995(May 2006).
17. P. Mészáros, *Reports on Progress in Physics* **69**, 2259(August 2006).
18. A. Pe'er, F. Ryde, R. A. M. J. Wijers, P. Mészáros and M. J. Rees, *Astrophys. J.* **664**, L1(July 2007).
19. B. Zhang and A. Pe'er, *Astrophys. J.* **700**, L65(August 2009).
20. H. Gao and B. Zhang, *Astrophys. J.* **801**, p. 103(March 2015).
21. A. Pe'er, H. Barlow, S. O'Mahony, R. Margutti, F. Ryde, J. Larsson, D. Lazzati and M. Livio, *Astrophys. J.* **813**, p. 127(November 2015).
22. P. Jakobsson, A. Levan, J. P. U. Fynbo, R. Priddey, J. Hjorth, et. al., *Astron. Astrophys.* **447**, 897(March 2006).
23. S. B. Cenko, D. A. Frail, F. A. Harrison, J. B. Haislip, D. E. Reichart, et. al., *Astrophys. J.* **732**, 29(May 2011).

24. A. Pe'er, B.-B. Zhang, F. Ryde, S. McGlynn, B. Zhang, R. D. Preece and C. Kouveliotou, *Mon. Not. R. Astron. Soc.* **420**, 468(February 2012).
25. V. Z. Golkhou and N. R. Butler, *Astrophys. J.* **787**, p. 90(May 2014).
26. S. E. Woosley, *Astrophys. J.* **405**, 273(March 1993).
27. M.-A. Aloy, J.-M. Ibáñez, J.-A. Miralles and V. Urpin, *Astron. Astrophys.* **396**, 693(December 2002).
28. B. J. Morsony, D. Lazzati and M. C. Begelman, *Astrophys. J.* **665**, 569(August 2007).
29. A. Mizuta and M. A. Aloy, *Astrophys. J.* **699**, 1261(July 2009).
30. D. López-Cámara, B. J. Morsony, M. C. Begelman and D. Lazzati, *Astrophys. J.* **767**, p. 19(April 2013).
31. A. M. Beloborodov, *Mon. Not. R. Astron. Soc.* **407**, 1033(September 2010).
32. A. M. Beloborodov, *Astrophys. J.* **764**, p. 157(February 2013).
33. I. Vurm and A. M. Beloborodov, *ArXiv e-prints* (June 2015).
34. B. Ahlgren, J. Larsson, T. Nymark, F. Ryde and A. Pe'er, *Mon. Not. R. Astron. Soc.* **454**, L31(November 2015).
35. A. Pe'er and E. Waxman, *Astrophys. J.* **628**, 857(August 2005).